Mon. Not. R. astr. Soc. (1976) **176**, 421–441.

INSTABILITIES OF KELVIN–HELMHOLTZ TYPE FOR RELATIVISTIC STREAMING

*B. D. Turland** *and P. A. G. Scheuer*

Mullard Radio Astronomy Observatory, Cavendish Laboratory, Madingley Road, Cambridge CB3 0HE

(Received 1976 February 9; in original form 1976 January 7)

SUMMARY

Some models of extragalactic radio sources require that energy is transferred from the nucleus to the radio components by relativistic streams, and it is pertinent to ask how much such streams would be spread out laterally and slowed down by entrainment of surrounding material. As a preliminary to attempting to understand such a situation we here investigate the Kelvin–Helmholtz instability at a tangential velocity discontinuity when the relative motion is relativistic, for values of the sound speed in the two fluids which may or may not be relativistic. We also consider the case where one half space is occupied by a collisionless gas of particles or photons, which therefore cannot be treated as a fluid. The principal result is that growing modes exist in all these cases; the growth rates of small perturbations have been calculated for a wide variety of parameters.

1. INTRODUCTION

This study of flow instabilities in a relativistic fluid was undertaken with a view to deciding how realistic are models of powerful radio sources in which energy is supplied continuously to the outer components by a beam or jet originating in the galactic nucleus (or quasar) (e.g. Rees 1971; Scheuer 1974; Blandford & Rees 1974). These sources consist typically of a compact radio component coincident with the optical object and bright radio features (' heads ') located at some distance on either side of the optical object. There may be further regions of diffuse emission—' tails ' to the heads and possibly a ' bridge ' connecting the various components. In Cygnus A, which has been studied in some detail, the nucleus produces only 0·25 per cent of the total flux density at 5 GHz, from a region less than 2 pc across (Kellermann *et al.* 1975); the heads are a few kiloparsecs across and 50 kpc from the nucleus (Hargrave & Ryle 1974). In only a few cases are compact features found between the nucleus and the heads.

In ' continuous-supply ' models it is postulated that energy is produced in the nucleus, possibly in the form of low-frequency electromagnetic radiation, or relativistic plasma accelerated to supersonic speed, and that a beam is formed. The energy in the beam is randomized in the head regions by interaction with the intergalactic plasma, producing relativistic electrons and magnetic field which give rise to the synchrotron emission observed. Beams or jets are susceptible to flow instabilities which cause them to dissipate much of their ordered energy. If such instabilities occur in the beams of continuous-supply models we might expect the

* Present address: Culham Laboratory, Abingdon, Oxford OX14 3DB.

beams to spread out over large angles and also to see enhanced radio emission from the lines of the beams. The observations of radio sources do not conform to either of these expectations.

In this paper we consider various modifications to existing stability theory which may be relevant in discussing the flow of energy in a radio source. In Section 2 previous work on the Kelvin–Helmholtz instability is reviewed briefly. In Section 3 we derive the dispersion relation for the stability of a tangential discontinuity between gases which may be relativistic (i.e. with $\kappa T/mc^2 > 1$) and have relative flow velocities approaching the speed of light, and show that there are always unstable modes. Numerical solutions of the dispersion relation are presented in Section 4 for cases of particular interest. In Section 5 a model is developed for the stability of a beam of low frequency electromagnetic radiation collimated by an external medium. It is shown that unstable modes occur in all cases and numerical results are presented in Section 5.3. The application of these results to the radio source problem is discussed briefly in Section 6.

2. THE KELVIN–HELMHOLTZ INSTABILITY

The Kelvin–Helmholtz instability (that of a tangential discontinuity between parallel flows) is one of the classic instabilities of fluid dynamics and has received wide attention. Linear perturbation analyses have been made for both incompressible and compressible fluids, finite free shear layers, free jets, and fluids containing magnetic fields, and useful reviews have been given by Chandrasekhar (1961), Gerwin (1968) and Southwood (1968). In particular, Miles (1958) and Fejer & Miles (1963) have considered the stability of a tangential discontinuity between inviscid fluids in situations where the relative flow velocity is of a magnitude similar to the sound speeds in the fluids (the compressible regime). With the assumption that the ratio of the specific heats is the same for both fluids, they deduce that the perturbations with wave vector $\mathbf{k}$ at an angle θ to the relative velocity are unstable for

$$U \cos\theta < (a_1{}^{2/3} + a_2{}^{2/3})^{3/2},$$

where U is the relative velocity, a_1 is the sound speed in fluid (1), a_2 is the sound speed in fluid (2), and thus conclude that unstable modes exist for all values of the relative velocity. If the ratio of specific heats is not the same in both media the results will be modified but, as demonstrated below, perturbations propagating sufficiently obliquely to the relative flow velocity will always be unstable.

A tangential discontinuity between incompressible fluids may be stabilized for small flow velocities by a magnetic field parallel to the flow in one fluid, or by unaligned fields in both fluids, the necessary conditions being given by Landau & Lifshitz (1960). In the compressible regime the situation is much more complicated and there seems to be no general agreement whether or not for certain field configurations there exists a critical flow velocity above which all perturbations are stable. The most comprehensive discussion is that given by Southwood (1968), who suspects that simultaneous stabilization for all values of θ is not possible.

The effect of considering a finite shear layer rather than a tangential discontinuity in the incompressible problem is to reduce the growth of perturbations whose wavelength is comparable to the thickness of the shear layer, shorter wavelengths being stable. The cylindrical geometry of a free jet is analogous to the planar geometry of a tangential discontinuity only if the wavelengths of the perturbations are much smaller than the radius of the jet. It seems probable that the regions of stability do not transform directly from the planar to the cylindrical geometry in the compressible regime (Gill 1965), although this effect is dependent on the geometry of the whole system and idealized models are suspect.

Most of the stability analyses have been performed from the temporal viewpoint; perturbations of the discontinuity with real $\mathbf{k}$ have been assumed and their behaviour with time has been investigated. For many problems though, the spatial approach (assuming real ω and investigating the growth or decay with distance) would appear to be a more realistic one, particularly in the study of jets for which the origin is fixed and quasi-periodic motions have been observed in the mixing region. The transformation between the two types of analysis is not obvious and the most suitable check is a direct comparison with experiments, which indeed seem to indicate that a spatial analysis is preferable (e.g. Mattingly & Chang 1974).

In spite of this we have restricted the analysis below to the temporal viewpoint; although the dispersion relation derived for the relativistic Kelvin–Helmholtz instability may be interpreted in terms of a spatial analysis, this is not true of the dispersion relation derived for the ' collisionless ' case in Section 5. The temporal analysis allows us to compare our results with those for compressibility alone and gives an indication of the importance of the instability with different sets of flow and fluid parameters. A fuller approach to the stability of relativistic jets would require direct computation of the initial value problem, but this does not seem worthwhile at present since the parameters of the models we are interested in are not well defined. Thus the following analysis gives us at best a feel for what might happen in the real situation where the effects of geometry, finite shear layers, magnetic fields and possible anisotropies may also be important.

3. A RELATIVISTIC TREATMENT OF THE KELVIN–HELMHOLTZ INSTABILITY

We consider the situation where either or both fluids may have relativistic sound speeds a_1, a_2, and the relative velocity U may be relativistic, but we apply small perturbations, so that the velocity in each fluid, relative to its own rest frame when unperturbed, is $v \ll c$. We assume that the effects of gravity and viscosity are negligible. We take the tangential velocity discontinuity as the x–y plane, with x in the direction of $\mathbf{U}$, and consider fluid (1) ($z > 0$) to be at rest.

The equations of motion and continuity can be summarized in the relationship (Synge 1955, Chapter 8)

$$\frac{\partial T_{\mathrm{rs}}}{\partial x_{\mathrm{s}}} = 0, \tag{3.1}$$

where

$$T_{\mathrm{rs}} = (\rho + P/c^2)\,\lambda_{\mathrm{r}}\lambda_{\mathrm{s}} + \delta_{\mathrm{rs}}P \tag{3.2}$$

is the energy-momentum tensor,

$$x_{\mathrm{s}} = (\mathbf{r}, ict), \quad \lambda_{\mathrm{s}} = [(1 - \mathbf{v}^2/c^2)^{-1/2}\,\mathbf{v}, (1 - v^2/c^2)^{-1/2}\,ic]$$

$$\rho = \text{proper density}, \quad \text{and} \quad P = \text{pressure}.$$

Since $v \ll c$ the equation may be written in the more usual three-vector forms

$$(\rho + P/c^2)(\partial \mathbf{v}/\partial t + (\mathbf{v}.\nabla)\mathbf{v}) = -\nabla P + (\mathbf{v}/c^2)\,\partial P/\partial t, \tag{3.3}$$

$$\partial \rho/\partial t + \nabla.((\rho + P/c^2)\,\mathbf{v}) = 0. \tag{3.4}$$

We shall consider perturbations of the form

$$\begin{aligned} \rho &= \rho_0 + \rho', \quad \rho' = \rho_1 \exp(-i\omega t) \exp i(kx+ly) f(z), \\ v_{x,y} &= v_{x0,y0} \exp(-i\omega t) \exp i(kx+ly) f(z) \\ v_z &= v_{z0}(z) \exp(-i\omega t) \exp i(kx+ly). \end{aligned} \tag{3.5}$$

When equations (3.3) and (3.4) are linearized and applied to perturbations of the form (3.5) they become

$$-i\omega(\rho_0 + P_0/c^2)\,v_x = -ik\rho'(\partial P/\partial \rho)_{\text{adiabatic}}, \tag{3.6}$$

$$-i\omega(\rho_0 + P_0/c^2)\,v_y = -il\rho'(\partial P/\partial \rho)_{\text{adiabatic}}, \tag{3.7}$$

$$-i\omega(\rho_0 + P_0/c^2)\,v_z = -\frac{\rho'}{f}\frac{\partial f}{\partial z}\left(\frac{\partial P}{\partial \rho}\right)_{\text{adiabatic}}, \tag{3.8}$$

$$-i\omega\rho' + (\rho_0 + P_0/c^2)(ikv_x + ilv_y + \partial v_z/\partial z) = 0. \tag{3.9}$$

Elimination shows that $f(z) = e^{-mz}$, where

$$m^2 = k^2 + l^2 - \omega^2/a^2, \quad a^2 = (\partial P/\partial \rho)_{\text{adiabatic}},$$

and

$$v_y = (l/k)\,v_x, \qquad v_z = (im/k)\,v_x. \tag{3.10}$$

The sign of m is chosen so that $f(z) \to 0$ as $|z| \to \infty$.

It remains to match the perturbations across the boundary between the two fluids ($z = 0$). This is achieved in the usual way by matching the amplitudes of the disturbances and equating the variation in pressure in each fluid at the interface. Fluid (1) is at rest; fluid (2) ($z < 0$) moves toward positive x at speed U. The transformation of wave number from the frame of fluid (2) to that of fluid (1) is a Lorentz transformation:

$$\begin{aligned} \omega_1 &= \gamma(\omega_2 + Uk_2), \quad & \omega_2 &= \gamma(\omega_1 - Uk_1), \\ k_1 &= \gamma(k_2 + U\omega_2/c^2), \quad & k_2 &= \gamma(k_1 - U\omega_1/c^2), \quad l_1 = l_2, \end{aligned} \tag{3.11}$$

where γ stands for $(1 - U^2/c^2)^{-1/2}$.

The values of ω_1, l_1, k_1 must match at the boundary, which will be of the form

$$z = \xi(x, y, t) = \xi_0 \exp(-i\omega_1 t) \exp i(k_1 x + l_1 y)$$

in the rest frame of fluid (1). Now for each fluid

$$\partial \xi/\partial t = v_z = (im/k)\,v_x,$$

so that (3.6) gives

$$i\omega\xi = \frac{-ima^2\rho'}{\omega(\rho_0 + P_0/c^2)}. \tag{3.12}$$

The pressure on the surface is invariant under the Lorentz transformation (3.11), so the matching of pressures gives

$$a_1{}^2\rho_1{}' = a_2{}^2\rho_2{}'. \tag{3.13}$$

We now divide (3.13) by ξ to obtain the dispersion relation and note that the values of ξ given by equation (3.12) with suffixes 1 and 2 are numerically equal since z-displacements are Lorentz invariant. Substituting for m_1, m_2 and ω_2 from equations (3.10) and (3.11), and noting that $\mathrm{Re}(m_1)$ and $\mathrm{Re}(m_2)$ must have opposite signs, we obtain

$$\frac{(\rho_{01}+P_0/c^2)\,\omega_1^2}{(k_1^2+l_1^2-\omega_1^2/a_1^2)^{1/2}}+\frac{(\rho_{02}+P_0/c^2)(\omega_1-Uk_1)^2\,\gamma^2}{(\gamma^2(k_1-U\omega_1/c^2)^2+l_1^2-\gamma^2(\omega-Uk_1)^2/a_2^2)^{1/2}} = 0. \quad (3.14)$$

Writing $|k| = (k_1^2+l_1^2)^{1/2}$,

$$V = \omega_1/|k|, \quad \cos\theta_1 = k_1/|k|,$$

$$\Gamma_1' = \rho_{01}a_1^2/P_0+a_1^2/c^2 = \Gamma_1+a_1^2/c^2,$$

$$\Gamma_2' = \rho_{02}a_2^2/P_0+a_2^2/c^2 = \Gamma_2+a_2^2/c^2, \quad (3.15)$$

(3.14) may be expressed in the form

$$\frac{\Gamma_1'(V/a_1)^2}{\{1-(V/a_1)^2\}^{1/2}}+\frac{\Gamma_2'[\gamma(V-U\cos\theta_1)/a_2]^2}{\{\gamma^2(\cos\theta_1-UV/c^2)^2+\sin^2\theta_1-[\gamma(V-U\cos\theta_1)/a_2]^2\}^{1/2}} = 0. \quad (3.16)$$

In the non-relativistic case this simplifies to the usual Kelvin–Helmholtz dispersion relation

$$\Gamma_1(V/a_1)^2\{1-(V/a_1)^2\}^{-1/2}+\Gamma_2[(V-U\cos\theta)/a_2]^2\{1-[(V-U\cos\theta)/a_2]^2\}^{-1/2} = 0. \quad (3.17)$$

Both (3.16) and (3.17) become equations of sixth degree for V when multiplied out. In (3.14), (3.16) and (3.17), the square roots in the denominators are multiples of m for the two fluids, and the value of each square root that has a positive real part must be taken to ensure that the perturbation diminishes for large $|z|$. Some roots of the sixth degree equation in V must be rejected because they do not satisfy the original equation with this condition; the remaining solutions will be called 'genuine solutions'. Solutions with real V lead to pure imaginary m and correspond to refraction of a sound wave at an angle of incidence (like the Brewster angle in optics) for which the reflection coefficient happens to vanish.

If $\cos\theta_1$ is sufficiently small, and we look for solutions with $V \ll \min(a_1, a_2)$, (3.16) approximates to

$$\Gamma_1' V^2/a_1^2+\Gamma_2'\gamma^2\left(\frac{V-U\cos\theta_1}{a_2}\right)^2 = 0, \quad (3.18)$$

which has solutions

$$V = U\cos\theta_1\left(1\pm i\,\frac{\Gamma_1'^{1/2}a_2}{\gamma\Gamma_2'^{1/2}a_1}\right)^{-1}. \quad (3.19)$$

Substituting back in equation (3.16) one finds that (3.19) make the numerators of the two terms equal and opposite, and the denominators squared are both close to $+1$ if

$$\cos\theta_1 \ll \min(a_1/U, 1/\gamma). \quad (3.20)$$

Subject to condition (3.20), expressions (3.19) are approximations to genuine solutions, for they satisfy (3.16) when one takes both square roots to have positive real parts.

We have thus shown that sufficiently oblique perturbations always give rise to a growing and a decaying mode; there is always an instability, in relativistic as in non-relativistic regimes. The physical reason is of course the same: the component of **U** along the surface corrugations has no effect on either fluid (since we have neglected viscosity), leaving an arbitrarily subsonic relative motion in the **k** direction in the rest frame of either fluid. We now estimate the importance of the instability in two cases of interest.

4. SOLUTIONS OF THE DISPERSION RELATION

4.1 *The flow of cold matter at relativistic speeds*

We suppose that a_1 and a_2 are comparable and $\ll c$, but U is relativistic, and again consider perturbations with $\cos\theta_1 \ll 1$. We look for solutions of the dispersion relation (3.16) with $|V| \ll c$. The squared denominator of the second term in (3.16) may be written

$$1-\frac{V^2}{c^2}+\gamma^2\left(\frac{V-U\cos\theta_1}{c}\right)^2-\gamma^2\left(\frac{V-U\cos\theta_1}{a_2}\right)^2.$$

With our assumptions, the second term in this expression is much less than the first, and the third much less than the fourth. Thus (3.16) is approximated by

$$\Gamma_1\frac{V^2}{a_1^2}\left(1-\frac{V^2}{a_1^2}\right)^{-1/2}+\Gamma_2\left(\frac{V-U\cos\theta_1}{a_2/\gamma}\right)^2\left\{1-\left(\frac{V-U\cos\theta_1}{a_2/\gamma}\right)^2\right\}^{-1/2}=0. \qquad (4.1)$$

This is equivalent to the non-relativistic equation (3.17) with a_2 replaced by a_2/γ. Provided that $\Gamma_1 = \Gamma_2$ we can use the results of Fejer & Miles (1963) which show that unstable perturbations exist for

$$U\cos\theta_1 < \{a_1^{2/3}+(a_2/\gamma)^{2/3}\}^{3/2}. \qquad (4.2)$$

When a_1 and a_2/γ are comparable, the maximum of $\mathrm{Im}(V)$ is comparable with either of these; when $\gamma \gg 1$ the growth rate has a sharp maximum near $\cos\theta_1 \simeq a_1/c$, $\mathrm{Re}(V) \simeq a_1$, the maximum growth rate being given by

$$\mathrm{Im}(V) = 2^{-4/3}3^{1/2}a_1^{1/3}(a_2/\gamma)^{2/3}. \qquad (4.3)$$

These relationships are not symmetrical with respect to a_1 and a_2, but that must be expected, for the angle θ changes under a Lorentz transformation in a way which depends on V. Thus the stability criterion cannot be transformed directly, but similar relationships obviously hold in the rest frame of fluid (2) with subscripts 1 and 2 interchanged.

4.2 *The flow of relativistic gases*

The speed of sound in a relativistic gas tends to $c/\sqrt{3}$ as the temperature is increased. For the situations we are envisaging in radio sources it is likely that this is the sound speed in at least one of the media. The dispersion relation (3.16) has been solved numerically for $a_1 = a_2$ and $\Gamma_1 = \Gamma_2$, and the results are given in Figs 1, 2 and 3. (For ultrarelativistic gases $\rho = u/c^2 = 3P/c^2$ and therefore $\Gamma_1' = \Gamma_2'$). In Fig. 1 the value of $\cos\theta_1$ below which unstable perturbations exist is plotted against γ, while in Fig. 2 the value of $\cos\theta_1$ at which the maximum of $\mathrm{Im}(V)$ occurs is plotted against γ. Fig. 3 shows the variation of $\mathrm{Im}(V)_{\max}$ with γ.

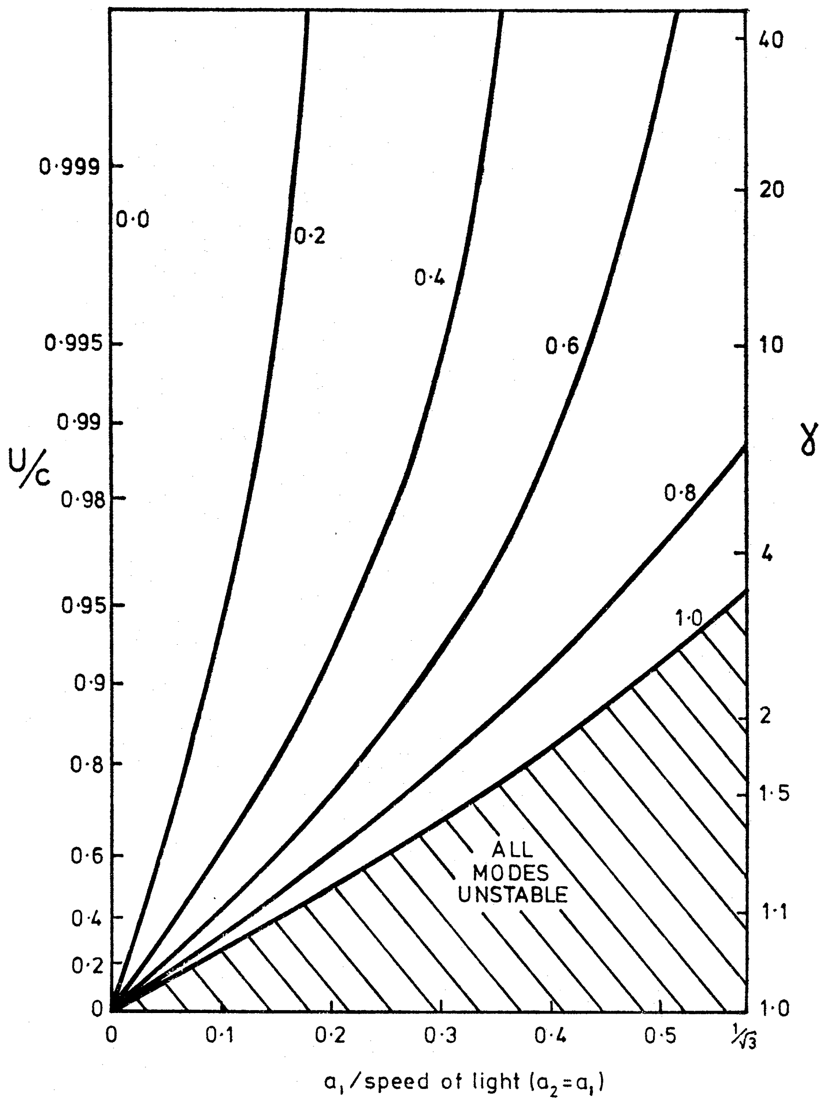

FIG. 1. *The value of cos θ below which there are unstable modes, when the sound speeds a_1 and a_2 in the two fluids are equal; θ is the angle between the wave vector and the velocity U of fluid* (2). *The vertical scale is linear in X such that $U/c = \tanh X$ and $\gamma = \cosh X$. (X is the ' angle of rotation ' in Minkowski space.)*

In Fig. 4, two examples of the dependence of Im(V) on cos θ are given, the extreme relativistic case showing a sharp maximum. The important perturbations at a given $|k|$ are those near cos θ where Im(V) is a maximum since these modes dominate in the linear regime and since it may be seen from Fig. 4 that the development of the disturbance is limited to a small range of cos θ if the flow is ultra-relativistic.

The numerical solutions show that, for relativistic flows in completely relativistic fluids, the maximum value of Im(V) $\simeq 0{\cdot}33c\gamma^{-0{\cdot}64}$ for $2<\gamma<512$ (which was the largest value of γ for which the growth rate was calculated). As shown in the Appendix the asymptotic expression for large γ is

$$\text{Im}_{\max}(V) \simeq 2^{-4/3}3^{1/2}(1-a_2^2/c^2)^{1/3}\, a_1^{1/3}(a_2/\gamma)^{2/3}. \qquad (4{\cdot}4)$$

The group velocity $\nabla_k\omega$ is of the order of U in all cases. For incompressible fluids Im(V) is of the same order of magnitude as U; from Section 4.1 it appears

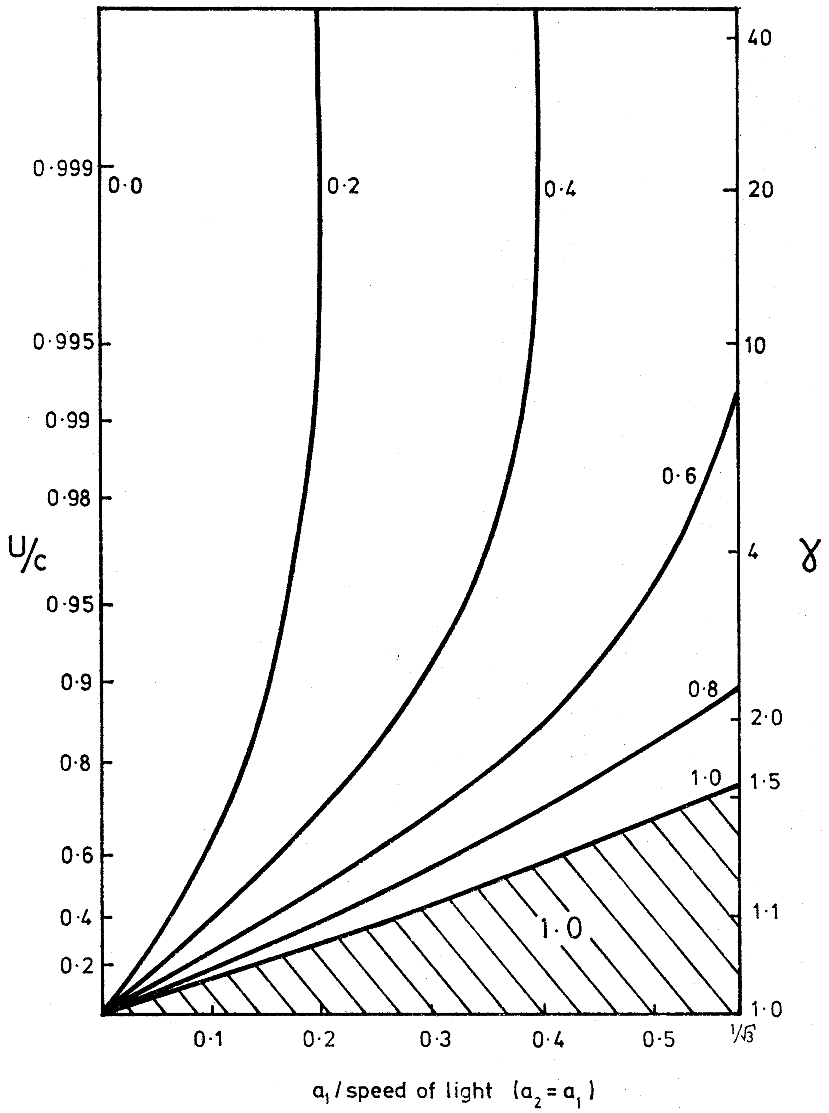

FIG. 2. *The value of cos θ for maximum instability.*

that Im(V) is of the order of the sound speed (or less if $\gamma \gg 1$) in hypersonic flow, and from this section it appears that Im(V) $\ll c$ even for relativistic sound speeds when $\gamma \gg 1$. Thus we may expect a wave packet to grow less in a given distance if the flow is relativistic than we should expect for a classical Kelvin–Helmholtz instability. We repeat that the spatial growth of a wave cannot properly be predicted using a group velocity in this way (*cf.* Section 2), and therefore we make the above remark cautious and qualitative.

4.3 *Mildly relativistic flow of relativistic gas over cool gas*

In the de Laval nozzle of Blandford & Rees' model, gas with sound speed $a_2 \simeq 3^{-1/2}c$ (or at any rate an appreciable fraction of c) flows, with a speed close to a_2, through a nozzle formed of much denser gas with sound speed $a_1 \ll c$. Therefore we have also investigated the regime in which a_2/c and γ are O(1) and $a_1 \ll c$. The methods are similar to those in the Appendix; the principal results are as follows: If

$$U \cos \theta < (a_2/\gamma)(1 - a_2^2/c^2)^{-1/2} \qquad (4.5)$$

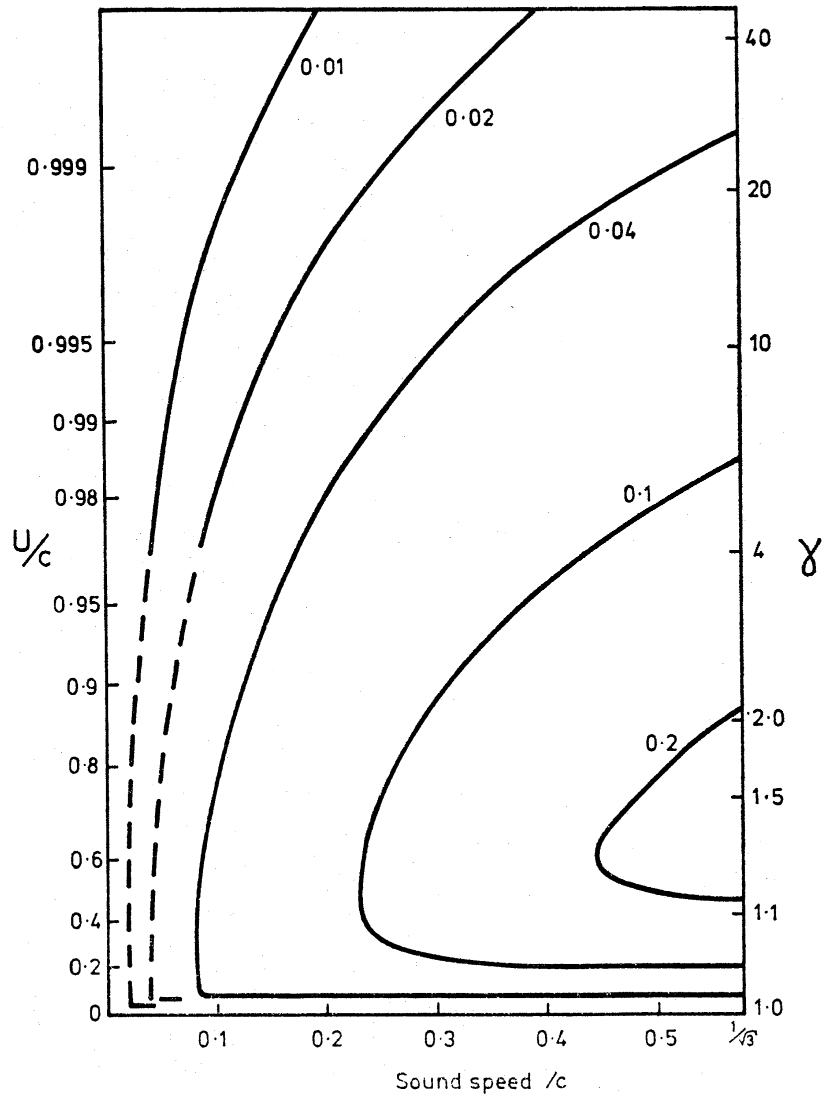

FIG. 3. *The growth rate at the maximum with respect to θ; the numbers in the diagram are* $Im_{max}(V/c)$.

by a margin $\gg a_1$, the dispersion relation (3.16) has two spurious real roots, two genuine real roots representing refracted sound waves, and two genuine complex roots. The complex roots are almost purely imaginary, and are approximately given by

$$(V/a_1)^2 = -\tfrac{1}{2}\Pi^2 - \tfrac{1}{2}\Pi(\Pi^2+4)^{1/2} \tag{4.6}$$

where

$$\Pi = (\Gamma_2'/\Gamma_1')(\gamma U \cos\theta/a_2)^2\{1-(\gamma U\cos\theta/a_2)^2(1-a_2{}^2/c^2)\}^{-1/2},$$

i.e. essentially the second term of the dispersion relation in the approximation $|V| \ll U\cos\theta$.

If, conversely,

$$U\cos\theta - (a_2/\gamma)(1-a_2{}^2/c^2)^{-1/2} \gg a_1, \tag{4.7}$$

the dispersion relation has six real roots, so that there is no growing mode.

As equation (4.6) shows, the largest growth rates occur when

$$U\cos\theta \simeq (a_2/\gamma)(1-a_2{}^2/c^2)^{-1/2},$$

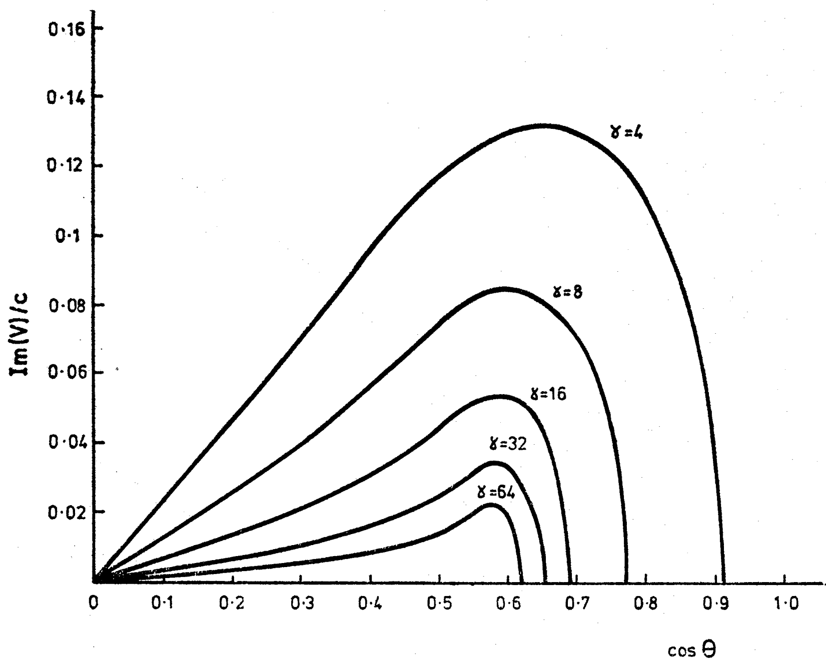

FIG. 4. *The variation of Im(V/c) with cos θ, for the case* $a_1 = a_2 = c/\sqrt{3}$ *and various values of* $\gamma = (1 - U^2/c^2)^{-1/2}$.

so that the denominator of the second term of (3.16) becomes small, and we must heed the presence of V in it. We then obtain a growing mode and a decaying mode, given approximately by the complex roots of

$$(V/V_0)^3 - B(V/V_0)^2 + 1 = 0 \qquad (4.8)$$

where

$$V_0{}^3 = \tfrac{1}{2}(\Gamma_2'/\Gamma_1')^2(U\cos\theta)^3(\gamma a_1/a_2)^2(1 - a_2{}^2/c^2)^{-1},$$

$$B = \{(1 - a_2{}^2/c^2) - (a_2/\gamma U\cos\theta)^2\}(a_2/\gamma a_1)^{2/3}(\Gamma_1'/2\Gamma_2')^{2/3}(1 - a_2{}^2/c^2)^{-2/3}.$$

The maximum growth rate (at fixed frequency) occurs when

$$U\cos\theta = (a_2/\gamma)(1 - a_2{}^2/c^2)^{-1/2}$$

and is given by

$$\mathrm{Im}_{\max}(V) = 2^{-4/3}3^{1/2}(\Gamma_2' a_1/\Gamma_1')^{2/3}(a_2/\gamma)^{1/3}(1 - a_2{}^2/c^2)^{-5/6}. \qquad (4.9)$$

Comparable growth rates occur over a range of the order of $(a_1/c)^{2/3}$ in $\cos\theta$.

Note that, if $U < (a_2/\gamma)(1 - a_2{}^2/c^2)^{-1/2}$, then condition (4.5) is satisfied for *all* θ; we then have a subsonic flow situation in which waves at all angles are unstable, with the maximum growth rate (given adequately by equation (4.6)) at $\theta = 0$.

5. BEAMS OF LOW FREQUENCY ELECTROMAGNETIC RADIATION

5.1 *Description of the problem*

We have demonstrated that a tangential discontinuity between inviscid fluids in the absence of gravity and magnetic fields leads to an Kelvin–Helmholtz instability, even if the relative velocities are comparable with the speed of light. We now consider if the above model is applicable to the stability of a surface between a plasma and a beam of low frequency electromagnetic radiation propagating in a tunnel blown out of the plasma. In this model, based on the discussion by Rees (1971), the frequency of the radiation is below the plasma frequency and thus the beam can only propagate in the tunnel. The system is considered in equilibrium, with external plasma pressure equal and opposite to the radiation pressure arising from glancing reflection of the radiation from the inner surface of the tunnel. In the rest frame of the plasma the radiation is anisotropic, carrying momentum and energy, and thus we have the possibility of a flow instability.

The low frequency radiation can be treated as a fluid only if the mean free path of the photons is short enough. Strong electromagnetic waves interact non-linearly in the presence of charged particles; the resulting scattering has been discussed by Max & Perkins (1972) and by Max (1973). Thus it is possible that a beam of very strong waves containing a little plasma could legitimately be treated as a fluid; it would have sound speed $3^{-1/2}c$, and the preceding analysis would apply. (' Strength ' here refers to the parameter $f = eE/mc\omega$, where E is the electric field of the wave and ω its angular frequency; if $f \gtrsim 1$ the radiation is called strong, if $f \ll 1$ it is called weak.) However, if the beam is in a good vacuum, or is weak, or both, the mean free path will be very large. To gain some insight into such situations we have investigated the case of a gas of ' photons ' with infinite free paths streaming past a fluid, and bouncing specularly off the interface.

If the mean free path is greater than the wavelength of the disturbance on the interface any pressure disturbances are quickly smoothed out in the collisionless gas of photons. Thus we may assume that the distribution of photons approaching the interface is constant, even if the reflected distribution is modified by a disturbance on the interface. This is not so in the fluid case and herein lies the essential difference between the two situations.

To study the stability of this collisionless system we again consider a boundary layer of zero thickness and plane geometry. We assume that the wavelength of the perturbations on the interface is much greater than the wavelength of a photon in the beam. (Parker (1958) used a similar model to discuss the interaction of the solar wind with the magnetosphere, treating the wind as collisionless particles, before it was generally recognized that MHD methods could be used.) The interaction of the radiation with the boundary will be complex, particularly if the radiation is strong, but if the initial beaming is good (i.e. $\langle\phi\rangle$ is small), reflection occurs after a change in refractive index $\phi^2/2$ for a photon initially making an angle ϕ with the interface and so the radiation need interact only with a small matter density $n = m\epsilon_0\omega^2/e^2 \langle\phi^2\rangle$. Because of multiple reflections we do not expect strong waves from a coherent source to be coherent in the cavity and therefore feel justified in applying the results of the statistical model developed below to models of radio sources in which energy is transported by strong waves.

5.2 *The dispersion relation for surface perturbations*

The plasma-filled half space is treated in the manner of Section 3; the pressure–amplitude relation for the photon beam is derived as follows.

The interface between the plasma and the beam ($z = 0$) is perturbed by a wave with z-displacement

$$\xi = \xi_0 \exp(-i\omega t) \exp i(|k|\, x \cos\theta + |k|\, y \sin\theta).$$

The photons are described by a distribution function $f(p, \Theta, \Phi)$, where p is the momentum of the photon, Θ is the angle its velocity makes with the x axis, Φ is the

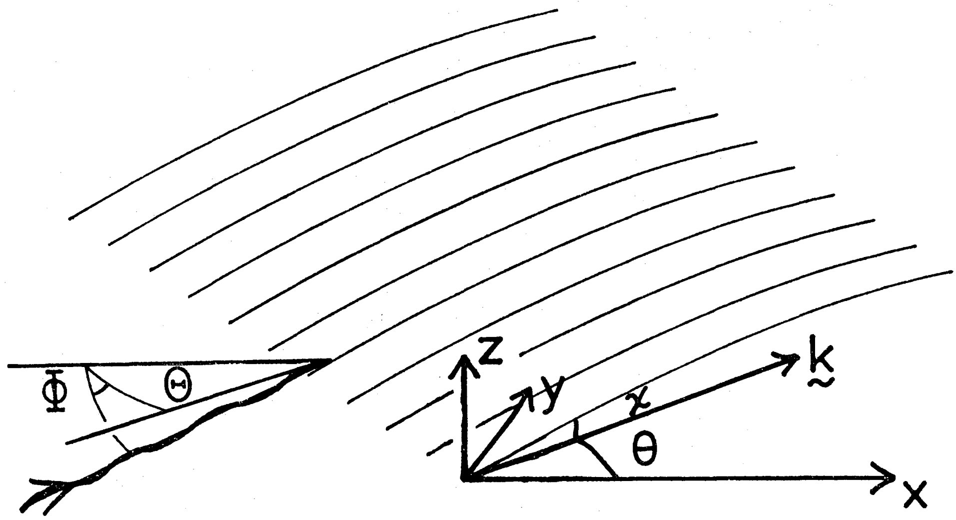

FIG. 5. *Reflection of a particle of the collisionless fluid at the interface with the collision dominated fluid.*

third spherical polar coordinate in momentum space, defined so that $\Phi = 0$ when $z = 0$. The perturbed interface makes angle χ with the $z = 0$ plane and therefore moves with speed $-V\chi$ in the z direction (see Fig. 5), where $V = \omega/|k|$.

With these definitions, the angle between an incident photon and the perturbed interface is α, where

$$\sin \alpha = \sin \Theta \sin \Phi - \chi(\cos \Theta \cos \theta + \sin \Theta \cos \Phi \sin \theta). \tag{5.1}$$

The quantities are now transformed into a frame moving with the instantaneous z velocity of the interface. Quantities in this frame are denoted by a prime.

On the assumption that the angle of incidence equals the angle of reflection, the radiation pressure on the interface is

$$P = P' = 2 \int_{\Phi=0}^{\pi} p_z' v_z' f' \, d^3\mathbf{p}'. \tag{5.2}$$

Now

$$p_z' = p' \sin \alpha' = p(\sin \alpha + V\chi/c) \tag{5.3}$$

(from the Lorentz transformation with $\gamma \simeq 1$),

$$f'(\mathbf{p}') = f(\mathbf{p}),$$

$$\frac{d^3\mathbf{p}'}{p'} = \frac{d^3\mathbf{p}}{p} \tag{5.4}$$

(Landau & Lifshitz 1971), and

$$v_z' = c \sin \alpha'.$$

Therefore

$$P = 2 \int_{\Phi=0}^{\pi} p' \sin \alpha' c \sin \alpha' f p' \, d^3\mathbf{p}/p$$

$$= 2 \int_{\Phi=0}^{\pi} p(\sin \alpha + V\chi/c)^2 \, cf \, d^3\mathbf{p} \qquad \text{by (5.3)},$$

and using (5.1) we find

$$P = P_0 - \chi C_1(C_2 \cos \theta - V/c), \tag{5.5}$$

where

$$\left.\begin{aligned} P_0 &= 2\int_{\Phi=0}^{\pi} pc \sin^2\Theta \sin^2\Phi f\, d^3\mathbf{p}, \\ C_1 &= 4\int_{\Phi=0}^{\pi} pc \sin\Theta \sin\Phi f\, d^3\mathbf{p}, \\ C_1C_2 &= 4\int_{\Phi=0}^{\pi} pc \sin\Theta \cos\Theta \sin\Phi f\, d^3\mathbf{p}, \end{aligned}\right\} \quad (5.6)$$

and we have assumed that

$$\int_{\Phi=0}^{\pi} pc \cos\Phi \sin\Phi \sin^2\Theta f\, d^3\mathbf{p} = 0. \quad (5.7)$$

The condition (5.7) is obviously true if the distribution of photon directions is symmetric about the xz plane; in other cases we can take the x axis along the mean flow direction defined by (5.7).

The parameter C_2 lies between 0 and 1; if the beam is well collimated, $\cos\Theta \simeq 1$ and $C_2 \simeq 1$.

If the angular distribution of photons is independent of their energy, i.e. if $f(p, \Theta, \Phi)/f(p, 0, 0)$ is independent of p, then

$$P_0 = \epsilon\langle\sin^2\Theta \sin^2\Phi\rangle \quad \text{and} \quad C_1 = 2\epsilon\langle\sin\Theta \sin\Phi\rangle, \quad (5.8)$$

where ϵ is the energy density in the beam (including reflected photons, see equation (5.6)), and $\langle\ \rangle$ denote averages over $0 < \Phi < \pi$.

The dispersion relation for perturbations of the interface between the beam and the plasma can now be derived by matching the pressures and amplitudes of the perturbation in the two media at the interface. Noting that $\chi = i|k|\,\xi$, and using the fluid treatment of Section 3 for perturbations in the plasma (which is taken to be at rest in the observer's frame), we find

$$C_1(C_2\cos\theta - V/c) = -iV^2(1 - V^2/a_1^2)^{-1/2}(\rho_0 + P_0/c^2) \quad (5.9)$$

where, as in (3.16), the square root with a positive real part must be taken to make the disturbance in the plasma fade away at great distances from the interface.

5.3 *Existence of an instability*

Defining Γ' for the plasma as in (3.15), the dispersion relation (5.9) may be written

$$g^{-2}(1 - V^2/a_1^2)(C_2\cos\theta - V/c)^2 + V^4/a_1^4 = 0 \quad (5.10)$$

where

$$\begin{aligned} g &= \Gamma' P_0/C_1 \\ &= \tfrac{1}{2}\Gamma'\langle\sin^2\Theta \sin^2\Phi\rangle/\langle\sin\Theta \sin\Phi\rangle \end{aligned}$$

if the angular distribution of photons is independent of energy; thus g is a mean glancing angle for the photons.

A necessary condition for all four roots of (5.10) to be real is that $C_2\cos\theta > a_1/c$. Thus for $\cos\theta < a_1/cC_2$ there is at least one root with positive imaginary part, corresponding to a growing mode, but before concluding that there is necessarily an instability we must check that the roots do indeed satisfy (5.9) when the square root is taken with positive real part. Numerical solutions of the dispersion relation (see below) indicate that the growing mode is a genuine solution of the physical problem and so the interface is unstable for all values of the parameters C_2, a and g.

If V/c can be neglected when compared with $C_2 \cos\theta$, the roots of (5.10) may be found directly and the condition for stable solutions only is that $C_2 \cos\theta > 2g$. At marginal stability ($C_2 \cos\theta = 2g$), $V = \sqrt{2a_1}$, and so for the original approximation to be valid we require $g \gg a_1/c$ (i.e. $a_1 \ll c\langle\Theta\rangle$). Thus, if $g \gg a_1/c$, modes with $C_2 \cos\theta < 2g$ are unstable, and this condition has been used as a check on the numerical solutions. The angle at which the growth rate, for given $|k|$, is a maximum is given by $C_2 \cos\theta = g$.

In Figs 6, 7 and 8 the results of numerical solutions of (5.9) are summarized—care was taken to exclude non-physical solutions. For all but the smallest values of g and the largest sound speeds, the maximum imaginary part of the phase velocity is a significant fraction of the sound speed, and thus there is always the prospect of significant instability.

Although we have used a different model from that employed in Sections 3 and 4 and obtained dissimilar dispersion relations, there is a noticeable similarity in the

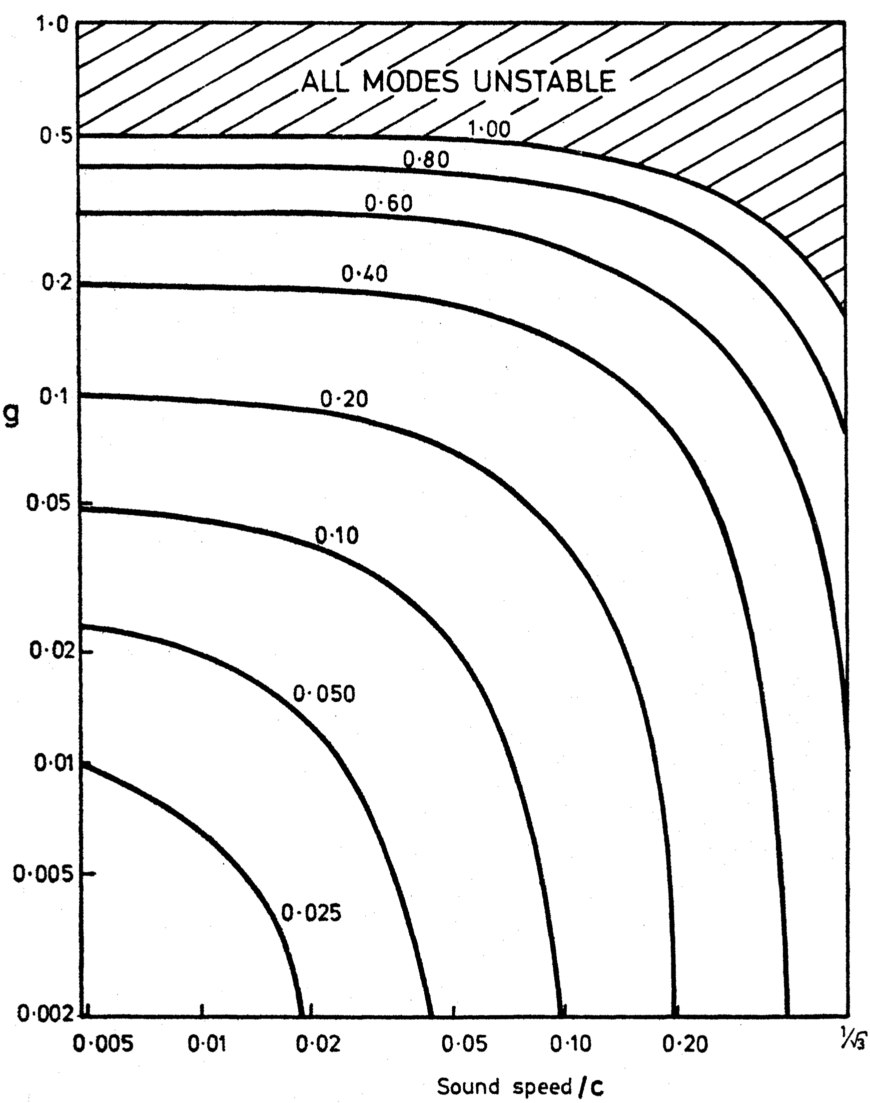

FIG. 6. *One fluid is collisionless: The value of $C_2 \cos\theta$ below which unstable modes exist.*

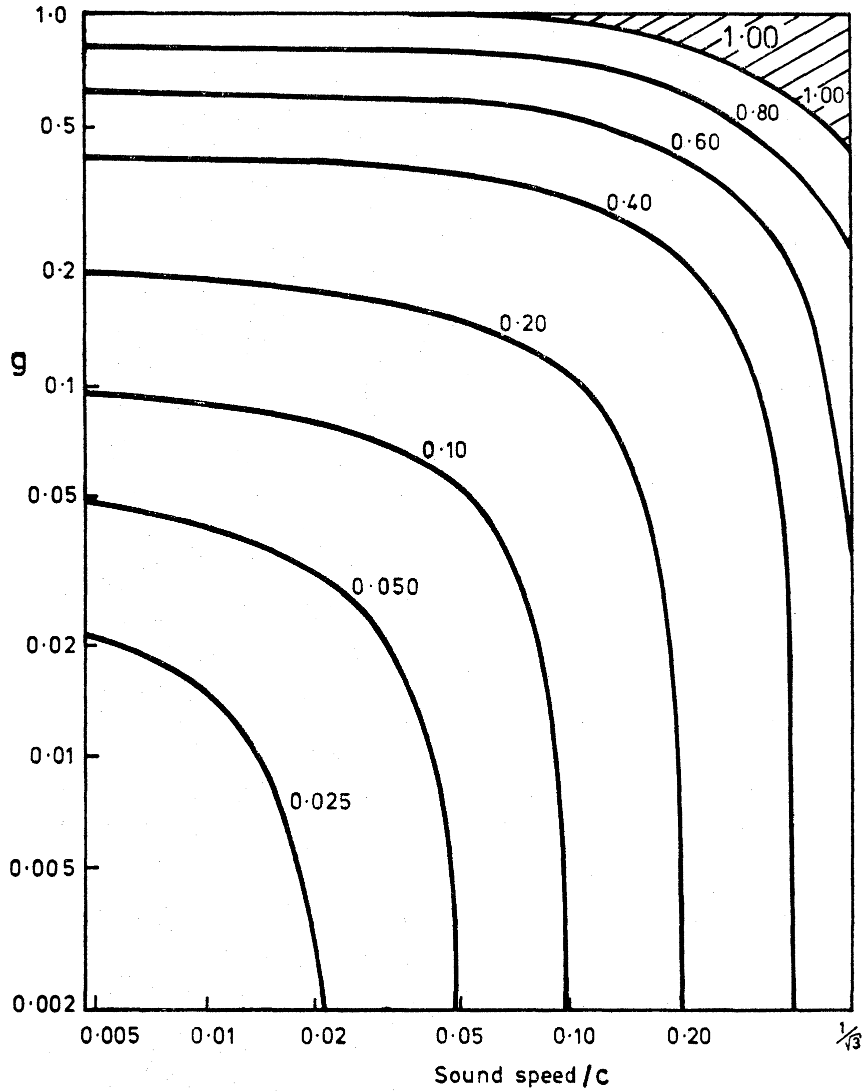

FIG. 7. *One fluid collisionless: The value of* $C_2 \cos \theta$ *for maximum instability.*

content of the numerical solutions. In particular the lowest growth rates may be achieved by having small sound speeds and either flow at high velocity of a well-collimated beam of radiation.

6. APPLICATION TO RADIO SOURCES

Before applying the above theory to radio source models we must, in principle, first decide which description (fluid or 'collisionless') is appropriate. In the regions of interest, however, both the nature of the unstable perturbations and their growth rates are similar (the latter to better than a factor of 3 if we compare the two descriptions by setting $a_2 = c/\sqrt{3}$, $\gamma = 1/g$), so there is no need to distinguish between them. Since the real situation may, in any case, lie somewhere between the two idealized models it is fortunate that the instabilities are so similar. Thus we always expect the development of a flow instability—the most unstable perturbations being parallel to the flow if the sound speeds are greater than or equal to the relative velocity ($c\langle\cos\Theta\rangle$ in the collisionless model), but oblique if the motion is

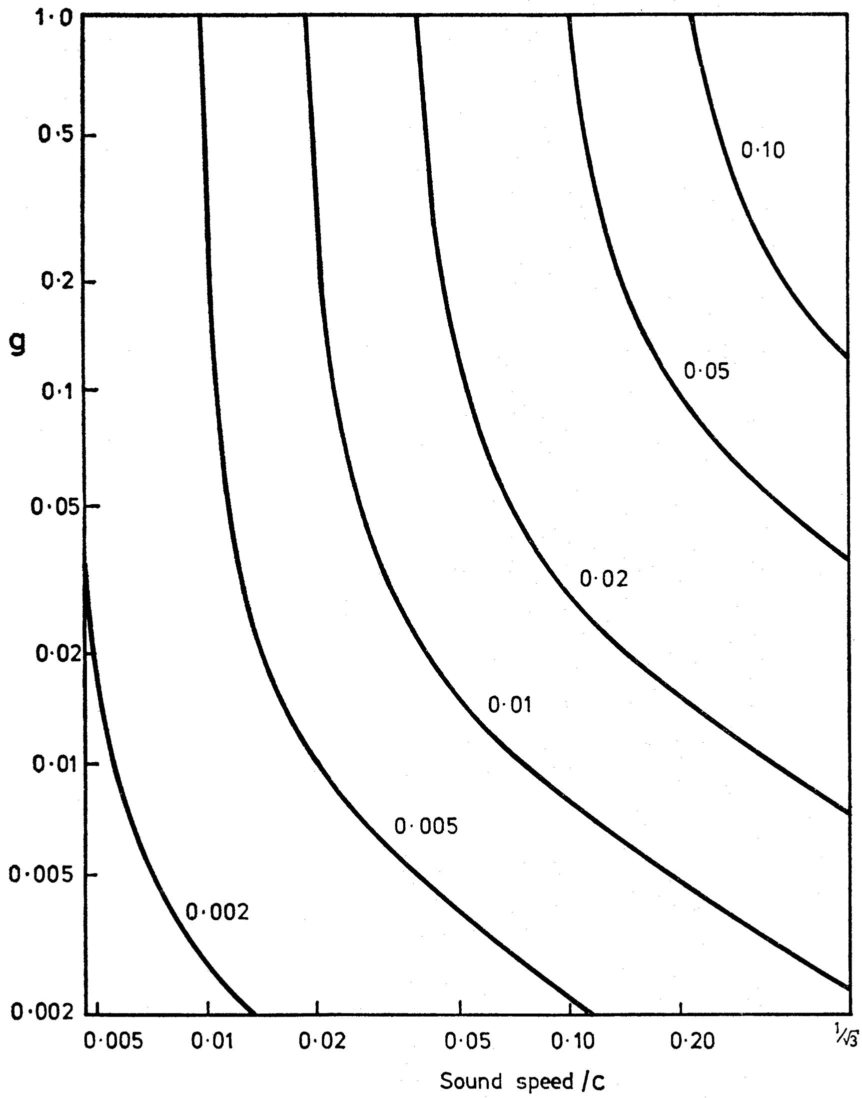

FIG. 8. *One fluid collisionless: The maximum value of Im(V/c).*

supersonic. As the relative velocity is increased, the values of cos θ for marginal stability (no growth) and for maximum instability tend to the ratio of the sound speed to the speed of light in both cases, but the growth rate of the most unstable perturbations is reduced (after passing through a maximum in the fluid case, the value of cos θ for maximum instability being close to 1).

In attempting to apply the results of linear perturbation analysis to the models of radio sources we might initially proceed as follows, guided to some extent by the behaviour of jets in laboratory conditions. We suppose that surface disturbances grow to amplitude $\sim k^{-1}$ and then decay into smaller eddies in a turbulent shear layer. Only perturbations of wavelength somewhat larger than the thickness of the shear layer will grow, so we are always concerned with the disturbance of the largest wavelength that has had time to grow to appreciable amplitude. We suppose that it is legitimate to think of a growing wave packet as moving along the jet with the group velocity (which is perhaps reasonable so long as the growth rate is smaller than the real part of the frequency) and, in all cases considered so far,* this is of

* Except the situation considered in Section 4.3, where the two fluids are extremely dissimilar.

the same order of magnitude as the relative velocity U. For a jet of length D and $\gamma \gg 1$ (as in the model of Blandford & Rees 1974), the time scale is D/c; while over a large region of parameter space, $\text{Im}_{\max}(V)$ lies between 0·01 and 0·1 c (Figs 3 and 8), so that the number N of e-folding times of modes with wavelength equal to the diameter d of the jet is

$$0{\cdot}01(2\pi D/d) < N < 0{\cdot}1(2\pi D/d).$$

The observed widths of the high-surface-brightness heads of the radio components give an upper limit for the width d of the postulated jet; the observations indicate that D/d is typically $\gtrsim 30$ and sometimes considerably greater. Thus there are probably enough e-folding times for perturbations on the scale of the jet to cause it to break up before it reaches the outer components. Our neglect of the finite thickness of the shear layer and of the cylindrical geometry introduces some uncertainty in our estimates of the growth rates. The growth rates would be reduced if (a) magnetic fields play an important part, or (b) the flow is highly relativistic but the sound speeds are low (good beaming). Thus a sound speed of 0·01 c ($T = 6 \times 10^8$ K) and $\gamma = 40$ (or $g = 0{\cdot}025$) leads to $\text{Im}_{\max}(V) \simeq 0{\cdot}003$ c, which in this simple-minded interpretation would not lead to disruption of the jet.

However, a number of serious complications have been ignored, including the following:

(i) If $U \gg (a_1, a_2)$ the growth of small-scale disturbances and their dissipation in a turbulent shear layer leads to an input of heat into that layer much greater than the initial thermal energy; therefore a shock will travel out into the surrounding gas and warm it up to such a temperature that a becomes comparable with U. Simple estimates indicate that the shock spreads faster than the instability, so that a strongly hypersonic regime never applies. Thus we probably should not appeal to the effect of hypersonic flow to save the stability of the beam.

(ii) It is far from clear how the turbulent shear layer develops when the primary surface corrugations are very oblique.

(iii) We can still use the relativistic nature of the flow (*cf.* Sections 4.1 and 4.2) to reduce the growth rates. But once entrainment of material around the jet begins to take place, the momentum of the jet is distributed over a larger mass, so the value of γ decreases; decreased γ increases the growth rates and therefore the entrainment rate is likely to increase very rapidly if it begins at all.

(iv) Divergence of the jet may be due in part to entrainment, but also in part to the diminution of ambient pressure with distance from the central massive object. While entrainment leads to a conversion of ordered into disordered energy, diverging supersonic flow leads to conversion of disordered into ordered energy. We do not know to what extent the latter may help to preserve the jet.

Thus we regard the work described here as a first step towards understanding the stability or instability of relativistic jets, but its predictive value for radio source models is limited.

7. CONCLUSIONS

We have derived and solved in particular cases the dispersion relation for

(a) the Kelvin–Helmholtz instability when relativistic effects become important, and

(b) the instability of a beam of electromagnetic radiation interacting with a half-space of plasma.

We have demonstrated that instability occurs for all values of sound speed and relative velocity (beaming parameter g) and that the two cases lead to remarkably similar results:

(i) that for low values of the relative velocity (poor beaming) the most unstable modes have **k** parallel to the relative velocity, and growth rates $\sim U|k|$ for (a) and $\sim a_1|k|$ for (b),

(ii) for high values of the relative velocity (good beaming) the most unstable mode has **k** oblique to the relative velocity, the parallel perturbations being stable,

(iii) for moderate relative velocities the compressibility of the fluids leads to a reduction in the growth rate of the perturbations below that expected for incompressible fluids, while relativistic flow ($\gamma \gg 1$, $g \ll 1$) leads to a further reduction,

(iv) for $\gamma \gg 1$ ($g \ll 1$) the value of $\cos\theta$ above which all modes are stable tends to a value near a_1/c, and the growth rate is sharply peaked at a slightly smaller value of $\cos\theta$.

We have tentatively applied these results to models of radio sources in which energy is continuously supplied from the nucleus to the outer components. If such models are to be physically acceptable we argue that the flow is probably highly relativistic, since the rate of growth of perturbations in the linear regime is lower than in the non-relativistic case.

REFERENCES

Blandford, R. D. & Rees, M. J., 1974. *Mon. Not. R. astr. Soc.*, **169**, 395.

Chandrasekhar, S., 1961. *Hydrodynamic and hydromagnetic stability*, Chapter XI, Clarendon Press, Oxford.

Fejer, J. A. & Miles, J. W., 1963. *J. fluid Mech.*, **15**, 335.

Gerwin, R. A., 1968. *Rev. mod. Phys.*, **40**, 652.

Gill, A. E., 1965. *Phys. Fluids*, **8**, 1428.

Hargrave, P. J. & Ryle, M., 1974. *Mon. Not. R. astr. Soc.*, **166**, 305.

Kellermann, K. I., Clark, B. G., Niell, A. E. & Shaffer, D. B., 1975. *Astrophys. J.*, **197**, L113.

Landau, L. D. & Lifshitz, E. M., 1960. *Electrodynamics of continuous media*, Article 53, Pergamon Press Ltd, Oxford.

Landau, L. D. & Lifshitz, E. M., 1971. *The classical theory of fields*, 3rd revised edition, Article 10, Pergamon Press Ltd, Oxford.

Mattingly, G. E. & Chang, C. C., 1974. *J. fluid Mech.*, **65**, 541.

Max, C. E., 1973. *Phys. Fluids*, **16**, 480.

Max, C. E & Perkins, F., 1972. *Phys. Rev. Lett.*, **29**, 1731.

Miles, J. W., 1958. *J. fluid Mech.*, **4**, 538.

Parker, E. N., 1958. *Phys. Fluids*, **1**, 171.

Rees, M. J., 1971. *Nature*, **229**, 312, 510.

Scheuer, P. A. G., 1974. *Mon. Not. R. astr. Soc.*, **166**, 513.

Southwood, D. J., 1968. *Planet Space Sci.*, **16**, 587.

Synge, J. L., 1955. *Relativity: the special theory*, Chapter 8—Article 14, p. 302, North-Holland Publishing Company, Amsterdam.

APPENDIX

THE KELVIN–HELMHOLTZ INSTABILITY WHEN $a_1 \gg a_2/\gamma$

The dispersion relation (3.16) can be written in the form

$$(V/a_1)^2\{1-(V/a_1)^2\}^{-1/2}+r\left(\frac{V-U\cos\theta}{a_2/\gamma}\right)^2 \times\left\{1-V^2/c^2-(1-a_2{}^2/c^2)\left(\frac{V-U\cos\theta}{a_2/\gamma}\right)^2\right\}^{-1/2}=0; \quad \text{(A1)}$$

where r is the ratio Γ_2'/Γ_1'. We shall refer to the two terms on the left-hand side of equation (A1) as $\mathrm{I} = (V/a_1)^2\{1-(V/a_1)^2\}^{-1/2}$ and $\mathrm{II} = r(\ldots)^2\{\ldots\}^{-1/2}$

Then *either*

(i) $|\mathrm{I}|$ and $|\mathrm{II}|$ are $O(1)$; this requires that $|V| = O(a_1)$ but V is not close to $\pm a_1$, and that $|V-U\cos\theta| = O(a_2/\gamma)$,

or

$|\mathrm{I}|$ and $|\mathrm{II}|$ are $\gg 1$; this requires

(ii) $V \simeq \pm a_1$,

or

(iii) $|V| \gg a$.

Cases (i), (ii) and (iii) are treated in turn below.

(i) Put $V = U\cos\theta+\epsilon$; we can neglect ϵ/a_1 in I but must keep terms in $\gamma\epsilon/a_2$ in II of (A1). We then get a quadratic equation in ϵ^2 whose solutions are

$$\gamma^2\epsilon^2/a_2^2 = (\mathrm{I}^2/2r^2)\{-(1-a_2^2/c^2)\pm[(1-a_2^2/c^2)^2+(4r^2/\mathrm{I}^2)(1-U^2\cos^2\theta/c^2)]^{1/2}\}. \tag{A2}$$

Thus we obtain four approximate roots of (A1), which will be discussed later. For the moment, we note only that the largest growth rates must be expected when I is large, i.e. in the present approximation when $U\cos\theta \simeq a_1$.

(ii) $V \simeq a_1$ (but $U\cos\theta$ is not close to a_1, in the sense that

$$|a_1-U\cos\theta| \gg a_2/\gamma).$$

Put $V = a_1(1+\epsilon)$; then (A1) is approximated by

$$(-2\epsilon)^{-1/2}+r\left(\frac{a_1-U\cos\theta}{a_2/\gamma}\right)^2\left\{(1-a_1^2/c^2)-(1-a_2^2/c^2)\left(\frac{a_1-U\cos\theta}{a_2/\gamma}\right)^2\right\}^{-1/2} = 0 \tag{A3}$$

and hence

$$\epsilon \simeq \tfrac{1}{2}(1-a_2^2/c^2)\,r^{-2}\left(\frac{a_1-U\cos\theta}{a_2/\gamma}\right)^2. \tag{A4}$$

This gives one real root; similarly another real root lies near $V = -a_1$. Thus cases (i) and (ii) between them supply all six roots of the squared form of (A1).

The above analysis breaks down for perturbations with $U\cos\theta \simeq a_1$, and they will be considered later.

(iii) $|V| \gg a_1$. Then either $|V-U\cos\theta| = O(a_2/\gamma)$, in which case we can use the approximations and obtain the result of case (i), or $|V-U\cos\theta| \gg a_2/\gamma$, in which case (A1) is approximated by

$$\pm iV/a_1 \pm ir\left(\frac{V-U\cos\theta}{a_2/\gamma}\right)(1-a_2^2/c^2)^{-1/2} = 0.$$

Therefore $|V-U\cos\theta| \ll |V|$ and again the approximation of case (i) can be used. Thus case (iii) yields no additional roots. Since only case (i) can yield complex roots for V, we consider it further.

(ia) $U\cos\theta < a_1$ and not close to a_1; $V = U\cos\theta+\epsilon$. Then I is real, and the square root in (A2) is real and its magnitude exceeds $(1-a_2^2/c^2)$. Therefore $\gamma^2\epsilon^2/a_2^2$ is real; we obtain two unphysical solutions (ϵ real) by taking the + sign in (A2) and two genuine solutions (ϵ pure imaginary) by taking the − sign in (A2).

If $U \cos \theta \ll c$, $a_2 \ll c$ and $r = 1$ the genuine solutions reduce to

$$\gamma^2 \epsilon^2 / a_2{}^2 \simeq -\left\{\left(\frac{a_1}{U \cos \theta}\right)^2 - 1\right\}^{-1}. \tag{A5}$$

(ib) $U \cos \theta > a_1$, but not close to a_1; $V = U \cos \theta + \epsilon$. Then $I^2 < 0$.
The expression under the square root in (A2) may be written

$$(1 - a_2{}^2/c^2)^2 - 4r^2(1 - a_1{}^2 U^{-2} \sec^2 \theta)\{a_1{}^2 U^{-2} \sec^2 \theta - a_1{}^2/c^2\}$$

whose least value occurs when $2a_1{}^2 U^{-2} \sec^2 \theta = 1 + a_1{}^2/c^2$ and is

$$(1 - a_2{}^2/c^2)^2 - r^2(1 - a_1{}^2/c^2). \tag{A6}$$

If expression (A6) is positive (in particular, if $\Gamma_1' = \Gamma_2'$ and $a_1 > a_2$) we get real values of the square root which are smaller than $(1 - a_2{}^2/c^2)$, and therefore obtain four real values of ϵ, representing genuine sound waves.

If the quantity (A6) is negative, either as a consequence of relativistic sound speeds or because $r > 1$, (A2) gives four complex values of ϵ over a certain range of $\cos \theta$ near $\cos \theta = a_1 U^{-1}\{\frac{1}{2}(1 + a_1{}^2/c^2)\}^{-1/2}$; owing to the approximation made in deriving (A2), I is not quite pure imaginary, and only two of the complex values of ϵ give genuine solutions; one is a growing and one a decaying mode.

Nothing analogous to these growing and decaying modes appears in Miles' (1958) or Fejer & Miles' (1963) treatment, as they assume $r = 1$ and strictly non-relativistic speeds throughout. These new modes have $Im(V)$ of the order of a_2/γ, since they occur for values of $U \cos \theta$ appreciably greater than a_1 and therefore $I = O(1)$. Thus their growth rates are smaller than the maximum growth rate of perturbations with $U \cos \theta = a_1$, given by (A10).

It remains to treat the case $U \cos \theta \simeq a_1$ (and the exactly similar case $U \cos \theta \simeq -a_1$). In that case, both $V \simeq U \cos \theta$ (case (i)) and $V \simeq a_1$ (case (ii)), but we cannot make the same approximations.

Put

$$V = U \cos \theta + \delta = a_1 + \xi + \delta$$

where ξ and δ are both $\ll a_1$. Then $|I| \gg 1$, hence

$$|II| \equiv |r\gamma^2 \delta^2 / a_2{}^2 \{\ldots\}^{-1/2}| \gg 1$$

and therefore *either* (ic)

$$\gamma \delta / a_2 \gg 1$$

or (id)

$$\{\ldots\} \ll 1.$$

In case (ic), (A1) is approximated by

$$\pm i \left(\frac{a_1}{2(\xi + \delta)}\right)^{1/2} \simeq \pm ri(\gamma \delta / a_2)(1 - a_2{}^2/c^2)^{-1/2}$$

which is a cubic equation for δ,

$$x^3 + Bx^2 - 1 = 0 \tag{A7}$$

where

$$\xi_0{}^3 \equiv \tfrac{1}{2} a_1 a_2{}^2 \gamma^{-2} r^{-2} (1 - a_2{}^2/c^2), \quad \delta \equiv x\xi_0, \quad \xi \equiv B\xi_0. \tag{A8}$$

Equation (A7) has two complex roots if $B < 3 \times 2^{-2/3}$.

Calling the real root of (A7) X, we can find a quadratic equation for the complex roots; the complex roots are

$$x = -\tfrac{1}{2}X^{-2} \pm (\tfrac{1}{4}X^{-4} - X^{-1})^{1/2} \tag{A9}$$

whose maximum imaginary part occurs when $X = 1$ $(B = 0)$ and is $\tfrac{1}{2}3^{1/2}$. Thus, using (A8),

$$Im_{\max}(V) = 2^{-4/3}3^{1/2}a_1^{1/3}(a_2/\gamma r)^{2/3}(1 - a_2^2/c^2)^{1/3} \tag{A10}$$

and growth rates of the same order of magnitude occur over a range $\sim \xi_0/U$ in $\cos\theta$. When B is large and negative, $X \simeq -B$ and (A9) approximates to the solution (A2) obtained earlier for case (ia).

In case (id),

$$1 - a_1^2/c^2 - (1 - a_2^2/c^2)\,\gamma^2\delta^2/a_2^2 \simeq 0$$

which gives two real values of δ, representing

2 unphysical real roots if $U\cos\theta + \delta < a_1$,

1 unphysical and 1 genuine real root if

$$U\cos\theta - \delta < a_1 < U\cos\theta + \delta,$$

2 genuine real roots if $U\cos\theta - \delta > a_1$.

The sixth root for V is a genuine real root near $V = -a_1$.

Many of the features described in the Appendix become clearer on sketching graphs of terms I and II as functions of real V in the various cases.